Supporting Information

Direct Growth of Three-Dimensional Nanoflower-like Structures from Flat Metal Surfaces

Jesse S. Dondapati [a], Maduraiveeran Govindhan [b] and Aicheng Chen [a]*

[a] Electrochemical Technology Centre, Department of Chemistry, University of Guelph, Guelph, ON N1G 2W1, Canada.

[b] Department of Chemistry, SRM Institute of Science and Technology, Kattankulathur 603 203, Tamil Nadu, India.

 * Corresponding author. E-mail: aicheng@uoguelph.ca

Experimental Section

Materials: Cobalt (Co) substrate (1.0 mm thickness, 99.95 purity), nitric acid (99.9%) were purchased from Sigma-Aldrich. All additional analytical grade reagents were of used as purchased. Pure water collected using a NANOpure® water system was employed in the preparation of all solutions. All electrochemical measurements were performed in 1.0 M KOH, as electrolyte solution.

Fabrication of Co_3O_4 nanoflowers: Initially Co substrates ($\sim$0.63 cm^2) were cleaned by sonication in acetone and then pure water. The Co_3O_4 nanoflowers on Co substrates were fabricated by placing a cleaned Co substrate electrode in 3 mL of 1.5 M nitric acid solution for a period of 5 h, 10 h, 17 h and 25 h at 50 ℃. A silicone oil bath was used to maintain constant temperature of 50 ℃. The resulting Co substrates were washed with copious amount of NANOpure water at room temperature and dried at 60 ℃ for 1 h. Co_3O_4 nanoflowers were formed on the etched Co substrate by annealing at 250 ℃, 350 ℃, 450 ℃ and 550 ℃ for 4 h in air with a ramp rate of 600 ℃/h and allowed to cool down by nature.

Characterization of nanomaterials: The fabricated nanostructured Co_3O_4 materials were characterized by using of various analytic techniques. The morphology and composition were characterized utilizing a field emission scanning electron microscope (FE-SEM) (Hitachi SU-70) equipped with the energy dispersive X-ray spectroscopy (EDX). The X-ray photoelectron spectra

were measured with a Thermo Fisher XPS system, where the size of the X-ray spot was 400 μm, using an Al Kα monochromatic source. Raman spectra were recorded using confocal micro-Raman spectroscopy with 514.5 nm laser excitation.

Electrochemical measurements: The electrochemical experiments were performed using of a Solartron SI 1287/1260 system employing a conventional one compartment three-electrode cell. A Co substrate (~0.63 cm^2) was employed as the working electrode, whereas a silver/silver chloride electrode (Ag/AgCl) was utilized as the reference electrode, and a platinum coil was used as the counter electrode. All electrochemical experiments were measured at ambient room temperature (20 ± 2 °C). All measured electrochemical potentials in this work against the Ag/AgCl electrode were converted to the reversible hydrogen electrode (RHE) scale for comparison with literature values based on Nernst equation as follows: $E_{RHE} = E_{AgCl} + 0.059(\text{pH}) + 0.197$ V. The results in the present study were not compensated for the internal resistance (iR). The onset potentials were calculated from the abscissa of intersection between the drawn tangents from non-faradaic and faradaic regions of LSV curve.
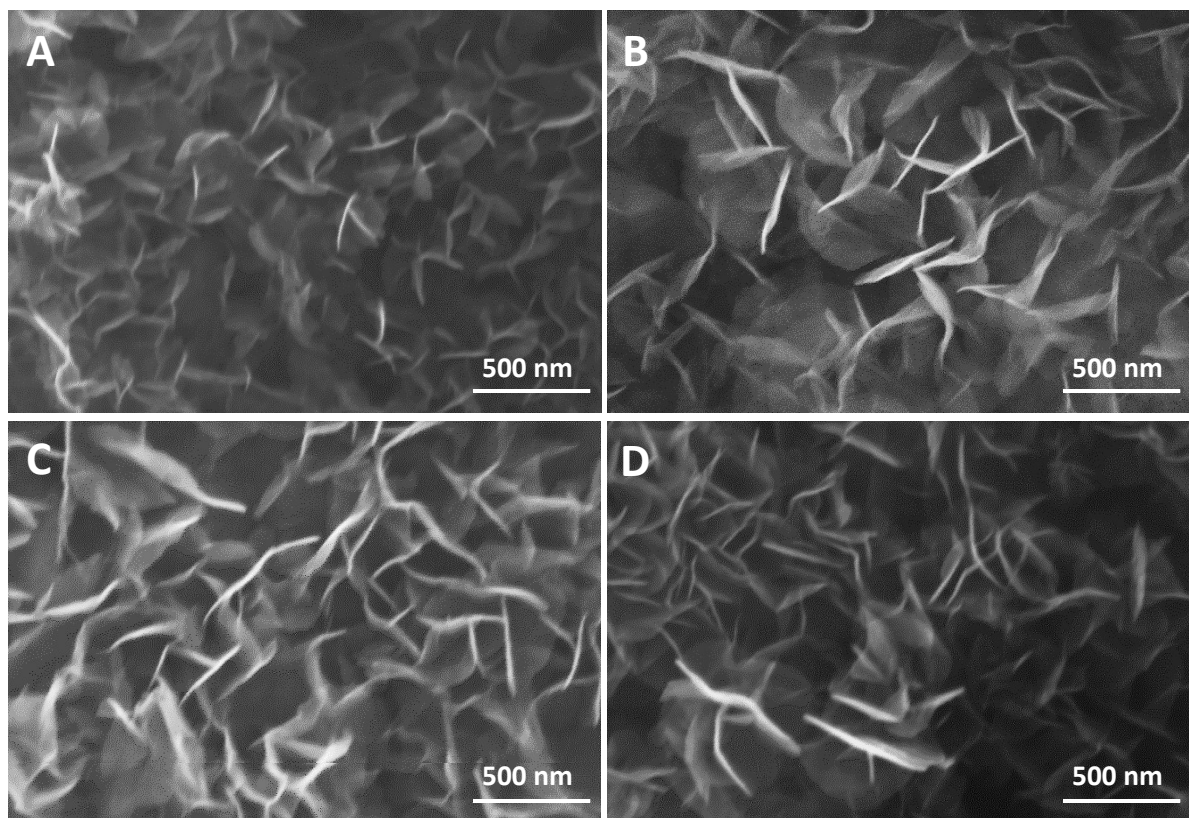
Figure S1: FE-SEM images of Co substrate treated in 1.5 M HNO$_3$ at 50 $^\circ$C for 5 h (A), 10 h (B), 17 h (C) and 25 h (D) showing the transforming morphology of nanoleaves with etching time (before annealing).
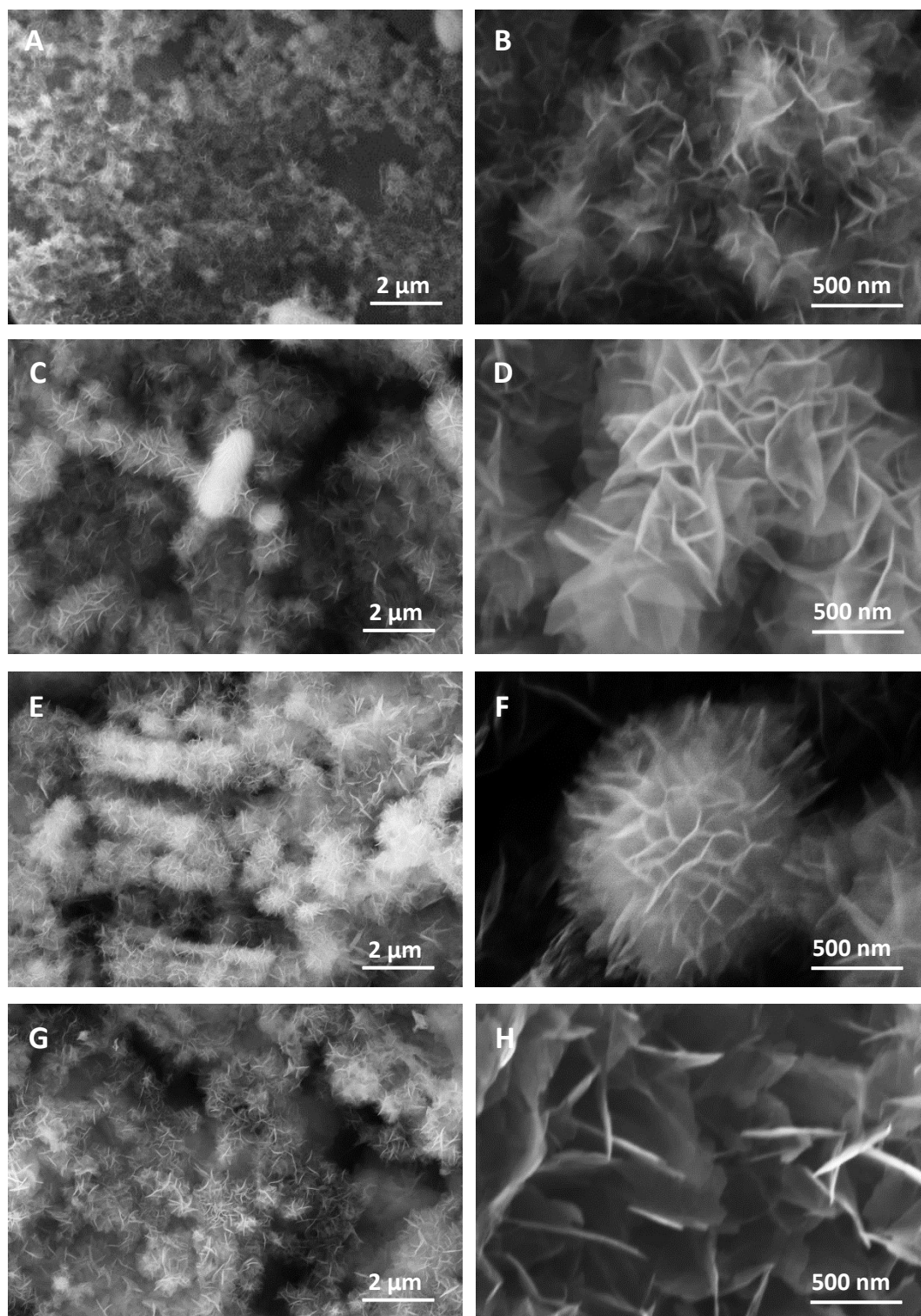
Figure S2: FE-SEM images of Co substrate treated in 1.5 M HNO$_3$ at 50 ℃ for 5 h (A & B), 10 h (C & D), 17 h (E & F) and 25 h (G & H) and annealed at 450 ℃.
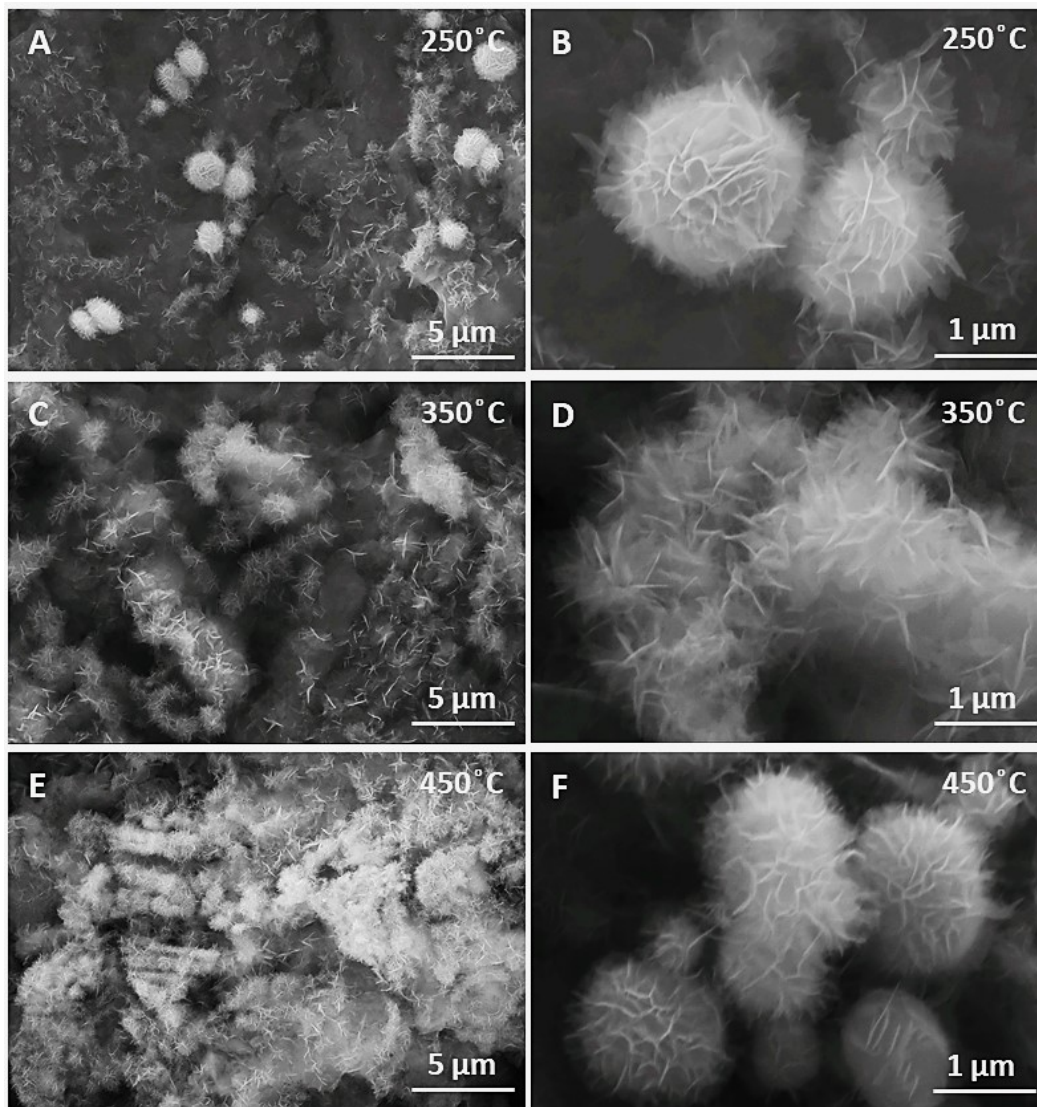
Figure S3: FE-SEM images of the Co_3O_4 nanomaterials formed by etching Co substrates for 17 h and annealing at temperatures of 250 ℃ (A & B), 350 ℃ (C & D) and 450 ℃ (E & F).
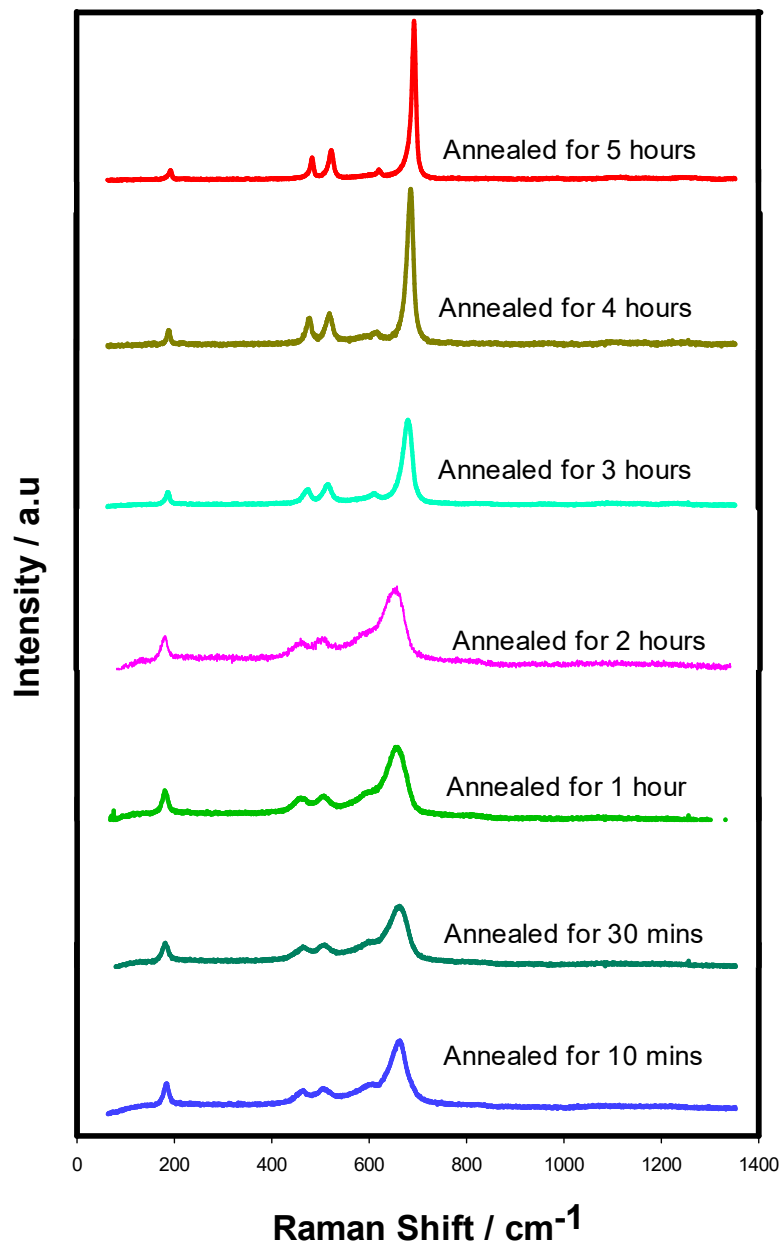
Figure S4: Raman spectra of Co plate sample that was etched for 17 hours and annealed from 10 mins to 5 hrs incrementally at 550 ℃.
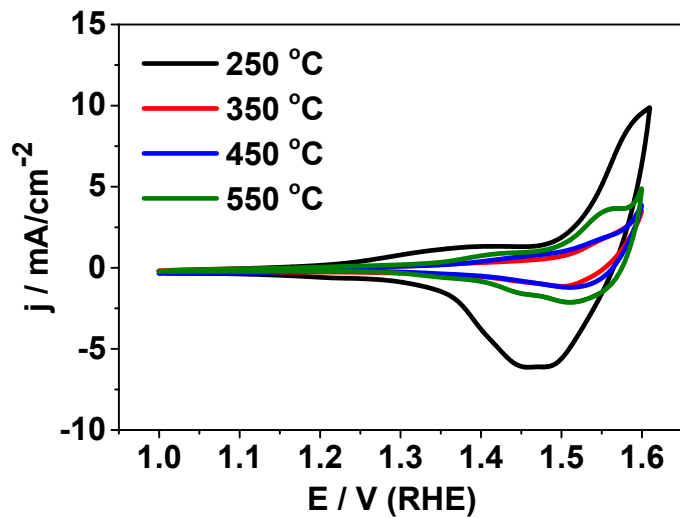
Figure S5: Cyclovoltammetry (CVs) of 17 hrs etched samples annealed at 250 ℃, 350 ℃, 450 ℃ and 550 ℃ recorded in 1 M KOH.
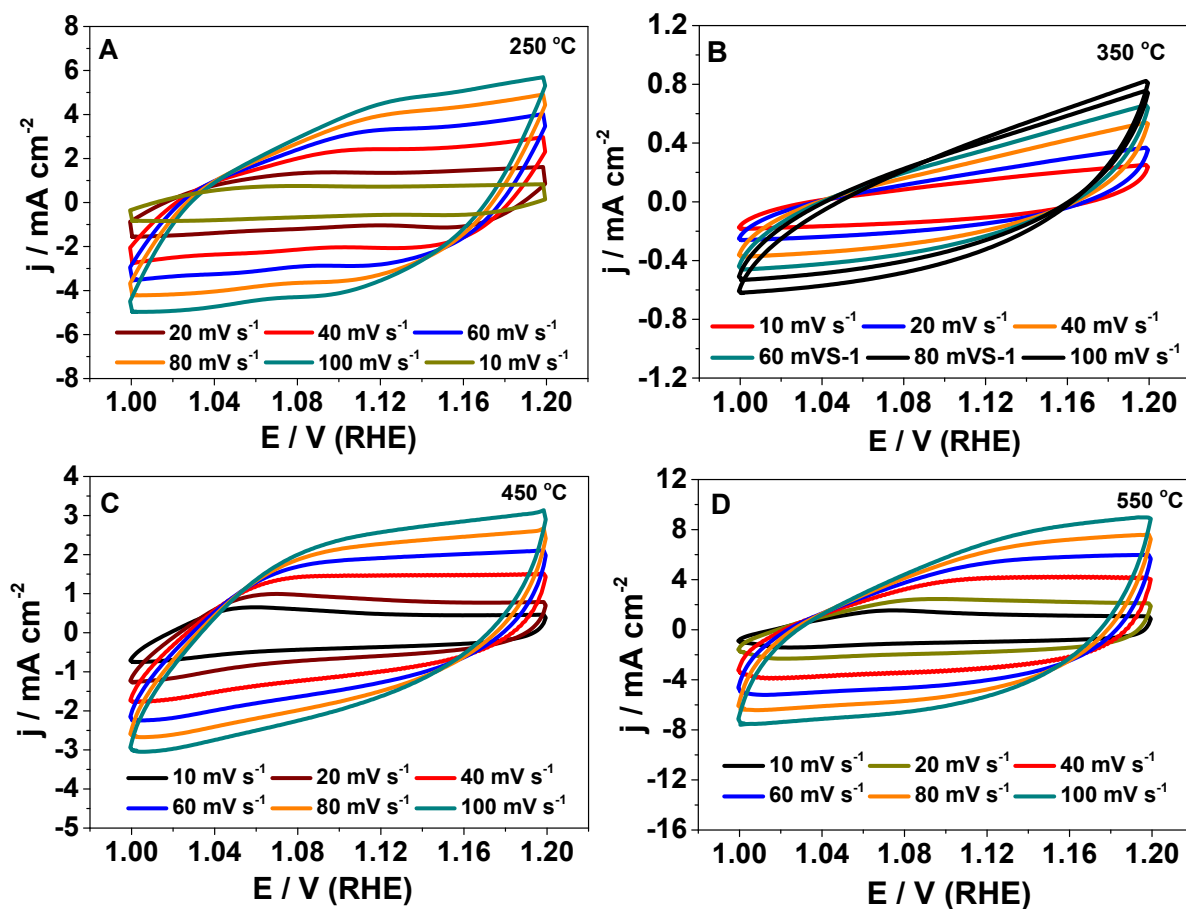
Figure S6: The electrochemical results of the formed Co$_3$O$_4$ nanoflowers on the bulk electrode surface in 1.0 M KOH electrolyte showing cyclovoltammetry (CV) tests recorded at increasing scan rates for electrodes annealed at 250 ℃ (A), 350 ℃ (B), 450 ℃ (C), 550 ℃ (D).
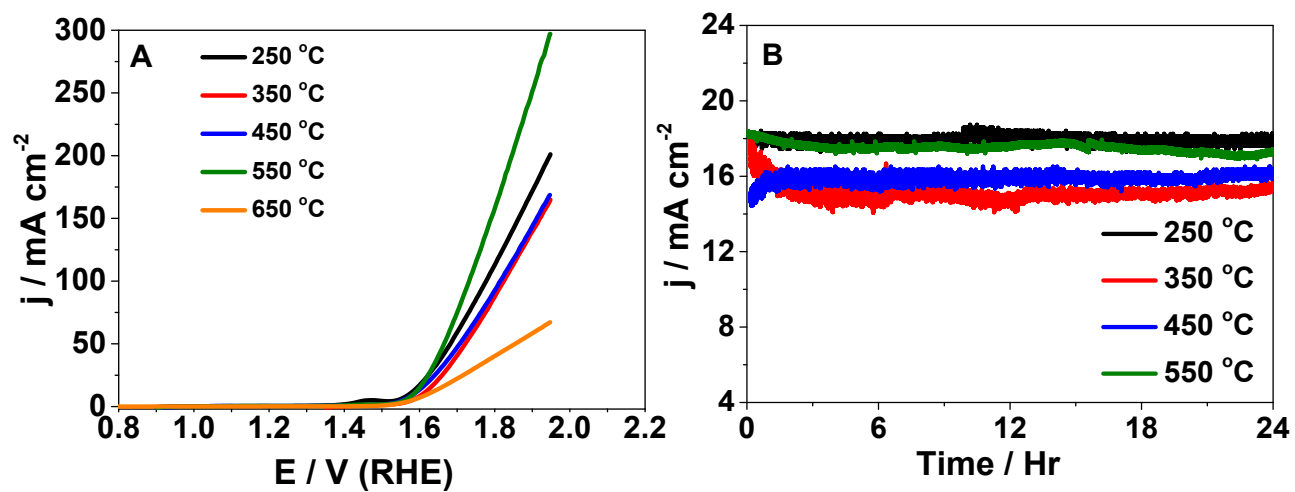
Figure S7: The linear sweep voltammetry (LSV) tests recorded at 5 mVs^{-1} (A) and the stability tests recorded for 24 h at 1.61 V (B).

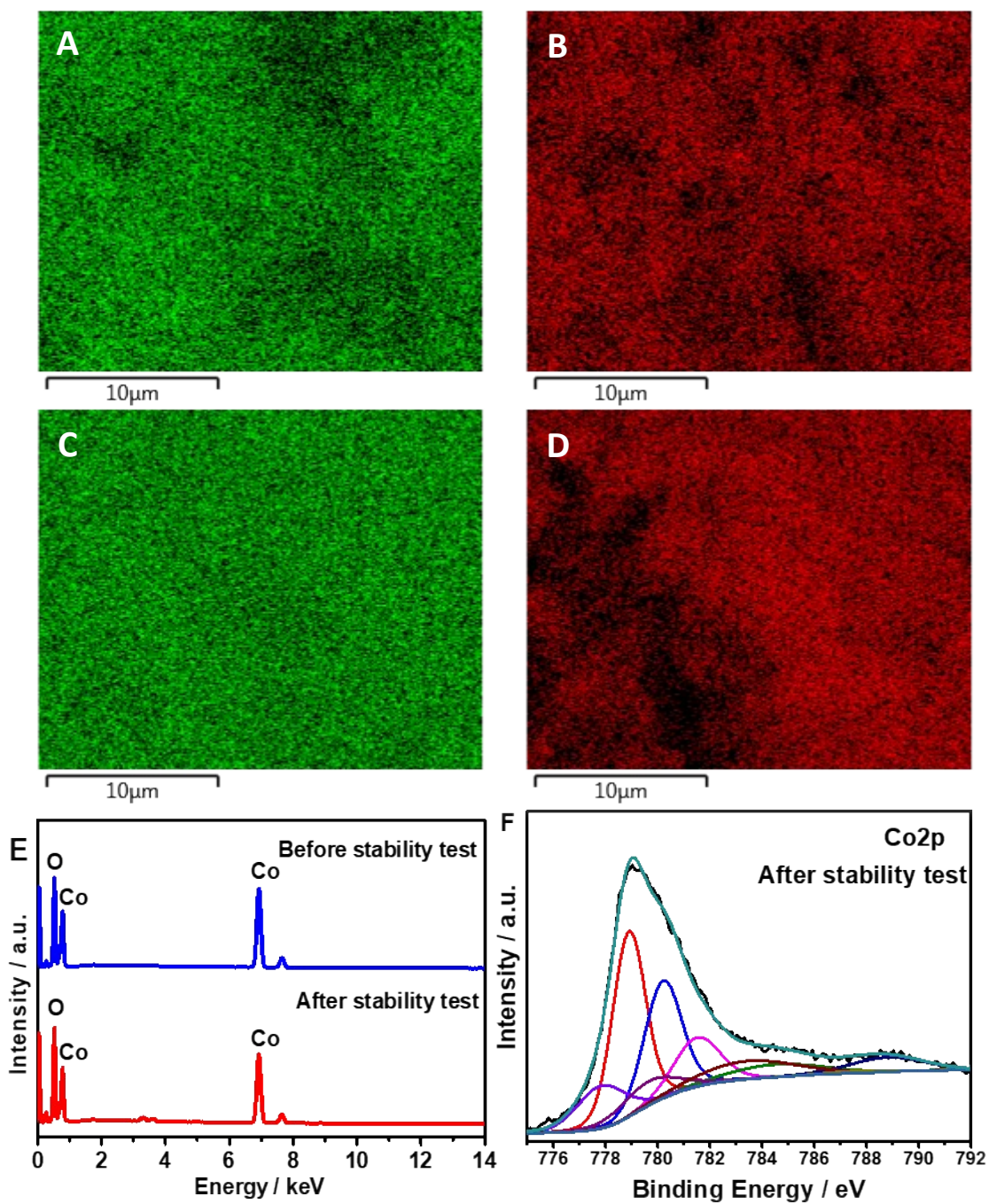**Figure S8:** EDX maps of the samples etched for 17 h and annealed at 550 °C for the elements Co (A) and O (B) before stability test; EDX maps of the same after stability test for elements Co (C) and O (D); The EDX spectra before and after the stability test (E); The XPS Co2p spectra after the stability test (F).
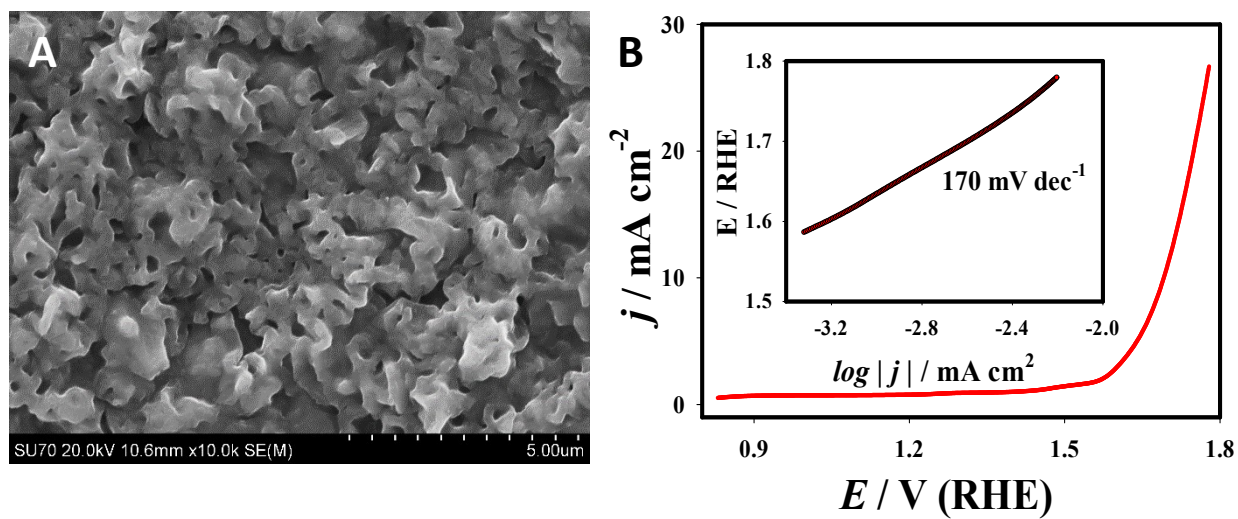
Figure S9: FE-SEM image of the Co substrate heated to 550 °C in air without treatment with nitric acid (A). LSV and Tafel plot (inset) of Co substrate directly annealed to 550 °C in air recorded in 1 M KOH (B).

Table S1. A list of dissolved mass of Co and corresponding morphological patterns of the Co substrate exposed in nitric acid.

Exposure Time (h)	Differences in Co substrate weights (mg)[a]	ICP-AES Dissolved Co mass (mg)	Leaf Length (Approx.)	Leaf Thickness (Approx.)	Co:O Ratio (EDX)
5	53.8	46.6	170 nm	15.4 nm	49.5: 50.5
10	52.8	55.8	230 nm	16.2 nm	36.7:63.3
17	53.0	56.0	230 nm	15.8 nm	27.4:72.5
25	53.3	53.5	350 nm	16.2 nm	26.5:73.5

[a] The differences in weights of Co substrates (~0.63 cm^2) prior to and following the etching process.

Table S2. The morphological parameters of the developed Co_3O_4 nanoflowers.

Annealing Temp (℃)	Flower Size (Approx.)	Leaf Length (Approx.)	Leaf Thickness (Approx.)	Co:O Ratio
250 ℃	2.1 μm	384 nm	6.9 nm	39.8:60.2
350 ℃	2.2 μm	326 nm	8.3 nm	36.2:63.8
450 ℃	1.6 μm	312 nm	9.3 nm	31.1:68.9
550 ℃	2.1 μm	240 nm	11.4 nm	26.8:73.2

Table S3. Comparison of Co_3O_4 nanoflowers formed at different annealed temperatures for the oxygen evolution reaction (OER) and other parameters.

Annealing Temp (℃)	OER Onset (V) RHE	Tafel Slope (mV.dec^{-1})	j at 1.69 V (mA.cm^{-2})	C_{dl} (mF.cm^{-2})
250 ℃	1.55	104	48	44.1
350 ℃	1.58	94	29	4.0
450 ℃	1.55	92	40	24.8
550 ℃	1.52	80	60	72.4

Table S4. A comparative table on performance of catalyst for OER with reported literatures

Catalyst	Electrolyte	Onset OER (V) (RHE)	η at 10 mA cm^{-2} (V)	Tafel Slope mV.dec^{-1}	Working electrode substrate	Loading mg cm^{-2}	Reference
CoQDs/rGO	0.1 M KOH	1.50	0.37	37.0	GCE	~0.008	S1
CoP	1.0 M KOH	1.56	0.49	59.0	GCE	~0.102	S2
*Co-N-GCI	0.1 KOH	-	0.43	69.0	GCE	0.5	S3
NiCoFeO$_4$	1.0 M KOH	1.50	0.38	50.5	Carbon paper	2	S4
NG-CoSe$_2$	1.0 M KOH	1.52	0.36	40.0	GCE	~0.2	S5
NiCoP/C	1.0 M KOH	1.51	0.33	96.0	GCE	-	S6
ZnCo$_2$O$_4$/ Co$_3$O$_4$	1.0 M KOH	1.52	0.39	46.0	Pt electrode	-	S7
Co$_3$O$_4$/NC-350	1.0 M KOH	1.51	0.30	69.0	GCE	-	S8
CoO-L	1.0 M KOH	1.59	0.37	46.0	Sustainable Coffee waste - hard template	1	S9
Co$_3$O$_4$/CoO	1.0 M KOH	1.53	0.30	68.6	Ti Foil	0.14	S10
Co$_3$O$_4$-NC/NGr-12 h	1.0 M KOH	1.43	0.28	69.0	GCE	0.05	S11
Co10-NS-C	1.0 M KOH	1.58	0.27	67.0	Ni Foam	-	S12
Co$_3$O$_4$-24 h	1.0 M KOH	1.45	0.30	67.7	Carbon paper	0.8	S13
Co$_3$O$_4$-550°C	1.0 M KOH	1.52	0.34	80.0	Bulk Cobalt	NA	This work

Co-N-GCI: cobalt and intercalated with conductive carbon nanospheres; NG: nitrogen doped graphene.

S1. Govindhan, M.; Mao, B.; Chen, A.; Novel cobalt quantum dot/graphene nanocomposites as highly efficient electrocatalysts for water splitting, *Nanoscale*, **2016**, *8*, 1485-1492

S2. Liu, M.; Li, J.; Cobalt Phosphide Hollow Polyhedron as Efficient Bifunctional Electrocatalysts for the Evolution Reaction of Hydrogen and Oxygen, *ACS Appl. Mater. Interfaces*, **2016**, *8*, 2158- 2165

S3. Qiao, X.; Liao, S.; Zheng, R.; Deng, Y.; Song, H.; Du, L.; Cobalt and Nitrogen Codoped Graphene with Inserted Carbon Nanospheres as an Efficient Bifunctional Electrocatalyst for Oxygen Reduction and Evolution. *ACS Sustain. Chem. Eng.,* **2016**, *4*, 4131 –4136.

S4. Maruthapandian, V.; Mathankumar, M.; Saraswathy, V.; Subramanian, B.; Muralidharan, S.; Study of the Oxygen Evolution Reaction Catalytic Behavior of $Co_xNi_{1-x}Fe_2O_4$ in Alkaline Medium, *ACS Appl. Mater. Interfaces* **2017**, *9*, 13132 –13141.

S5. Gao, M-R.; Cao, X.; Gao, Q.; Xu, Y-F.; Zheng, Y-R.; Jiang, J.; Yu, S-H.; Nitrogen-doped graphene supported $CoSe_2$ nanobelt composite catalyst for efficient water oxidation, *ACS Nano*, **2014**, *8*, 3970-3978.

S6. He, P.; Yu, X-Y.; Lou, X. W.; Carbon-Incorporated Nickel-Cobalt Mixed Metal Phosphide Nanoboxes with Enhanced Electrocatalytic Activity for Oxygen Evolution, *Angew. Chem. Int. Ed*. **2017**, *56*, 3897- 3900.

S7. Kim, T. W.; Woo, M. A.; Regis, M.; Choi, K-S.; Electrochemical Synthesis of Spinel Type $ZnCo_2O_4$ Electrodes for Use as Oxygen Evolution Reaction Catalysts, *J. Phys. Chem. Lett*. **2014**, *5*, 2370-2374.

S8. Zhang, J.; Qian, B.; Sun, S.; Tao, S.; Chu, W.; Wu, D.; Song, L.; Ultrafine Co_3O_4 Nanoparticles within Nitrogen-Doped Carbon Matrix Derived from Metal-Organic Complex for Boosting Lithium Storage and Oxygen Evolution Reaction, *Small*, **2019**, 15, 1904260

S9. Yu, M.; Waag, F.; Chan, C. K.; Weidenthaler, C.; Barcikowski, S.; Tuysuz, H.; Laser Fragmentation-Induced Defect-Rich Cobalt Oxide Nanoparticles for Electrochemical Oxygen Evolution Reaction, *ChemSusChem*, **2020**, 13, 520-528.

S10. Liu, Z.; Xiao, Z.; Luo, G.; Chen, R.; Dong, C-L.; Chen, X.; Cen, J.; Yang, H.; Wang, Y.; Su, D.; Li, Y.; Wang, S.; 2D Fe-doped NiO nanosheets with grain boundary defects for the advanced oxygen evolution reaction, *Small*, 2019, 15, 1904903.

S11. Singh, S. K.; Dhavale, V. M.; Kurungot, S.; Low Surface Energy Plane Exposed Co_3O_4 Nanocubes Supported on Nitrogen-Doped Graphene as an Electrocatalyst for Efficient Water Oxidation, *ACS Appl. Mater. Interfaces*, **2015**, 7, 1, 442–451.

S12. Chaugule, A. A.; Mane, V. S.; Bandal, H. A.; Kim, H.; Kumbhar, A. S.; Ionic Liquid-Derived Co_3O_4-N/S-Doped Carbon Catalysts for the Enhanced Water Oxidation, *ACS Sustainable Chem. Eng.*, **2019**, 7, 17, 14889–14898

S13. Paul, B.; Bhanja, P.; Sharma, S.; Yamauchi, Y.; Alothman, Z. A.; Wang, Z-L.; Bal, R.; Bhaumik, A.; Morphologically controlled cobalt oxide nanoparticles for efficient oxygen evolution reaction, J. Colloid Interface Sci.**2021**, *582*, 322-332.